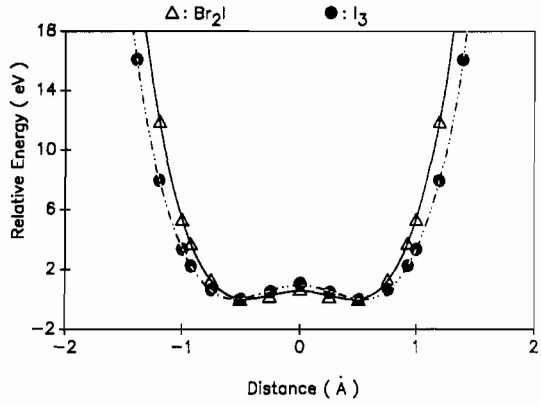

Figure 5. Charge-oscillation barrier heights in I_3^- and IBr_2^-.

site and the other characteristic of an Fe^{III} site. As the temperature is increased, the two doublets move together with no line broadening to become a single doublet above 280 K. If the intramolecular electron transfer in **16** was slower than the Mössbauer time scale (rate $< \simeq 10^7$ s^{-1}) at low temperature and then increased with increasing temperatures, the line widths of each doublet would be expected to broaden as the electron-transfer rate goes through the ^{57}Fe Mössbauer window. Absence of line broadening in Mössbauer spectra has been noted for **2-5**.[5] It has been concluded that the process which leads to the averaging seen in Mössbauer studies occurs at a rate faster than the Mössbauer time scale at all temperatures.

Micromodulation of Rate of Intramolecular Electron Transfer. The goal of this section is to present an explanation for the pronounced influence that the anion has on the rate of intramolecular electron transfer in mixed-valence biferrocenium salts. In Hendrickson's theoretical model,[12] the factors that are potentially important in controlling the rate of intramolecular electron transfer in the mixed-valence biferrocenium cation include (1) the effective barrier for electron transfer in the cation, (2) the effective barrier for charge oscillation in the anion, and (3) the intermolecular cation-cation and cation-anion interactions. In general, it has been suggested that the greater the effective barrier for charge oscillation in the cation or anion, the smaller the electron-transfer rate. Furthermore, the electron-transfer rate will be decreased with increasing cation-anion interaction.

Possible origins of the effect of replacing I_3^- by IBr_2^- in mixed-valence biferrocenium salts can now be proposed. From the theoretical calculations (Figure 5), the IBr_2^- anion could have a smaller barrier for charge oscillation than does the I_3^- anion. This would explain why the mixed-valence biferrocenium dibromoiodide has an electron-transfer rate in excess of 10^7 s^{-1} at a temperature 150 °C lower than that observed for biferrocenium triiodide.

Replacing I_3^- by IBr_2^- for mixed-valence 1',6'-diethyl- and 1',6'-diiodobiferrocenium cations has the opposite effect; the rate of electron transfer is reduced at a given temperature. The X-ray structure of **6**[28] reveals that in each stack of anions and cations there is an appreciable interaction between the terminal atoms of the I_3^- anions and the iodine atom on the Cp ring of the cation. Thus, there is a larger in-stack cation-anion interaction in the IBr_2^- salt than in the I_3^- salt. The increased cation-anion interaction in the IBr_2^- salt effectively reduces the rate of intramolecular electron transfer. The same could be happening in **15**. In fact, from the X-ray structure of **2**, Sano reported that there is a significant cation-anion interaction (3.78 Å) in this compound. Because the terminal bromine atoms in IBr_2^- carry more net negative charge than the terminal iodine atoms of I_3^-, the interaction between the terminal bromine and cation would be greater than the analogous interaction in the I_3^- salt. The increased cation-anion interaction in the IBr_2^- salt **15** also reduces the rate of electron transfer.

Conclusion

In this paper, we demonstrate that relatively minor perturbations caused by interactions with neighboring cations and anions in biferrocenium salts experiencing weak or moderate electronic coupling between two Fe centers have pronounced effects on the electronic structure and rate of intramolecular electron transfer. Furthermore, the influence of the nonzero zero-point energy difference on the rate of intramolecular electron transfer appears to be quite pronounced in compounds **9-13**.

Acknowledgment. We are grateful for support from the National Science Council (TYD).

Contribution from the Department of Chemistry, College of Arts and Sciences, The University of Tokyo, 3-8-1 Komaba, Meguro-ku, Tokyo 153, Japan

X-ray Diffraction and Electric Dichroism Studies on the Adsorption of Metal Complexes by a Clay

Masahiro Taniguchi, Akihiko Yamagishi,* and Toschitake Iwamoto

Received October 16, 1989

The binding structures of enantiomeric and racemic $[M(phen)_3]^{2+}$ (M = Ru, Fe; phen = 1,10-phenanthroline) complexes with sodium montmorillonite were studied by means of X-ray diffraction and electric dichroism measurements. The electron density curves along the *c* axis of a clay layer were determined for the powder samples of clay-chelate adducts. At maximum adsorption, the enantiomeric and racemic chelates formed the single-molecular and double-molecular layers in the interlayer spaces, respectively. The reduced linear dichroisms for the two characteristic bands in their electronic absorption spectra (i.e. the metal-to-ligand charge-transfer band at 400-500 nm and the ligand excitation bands at 240-280 nm) were determined for the bound metal complexes in a colloidal state. The orientation of a bound complex was elucidated by comparing the observed reduced linear dichroism with the ones calculated for the possible bound state in the interlayer space of a clay. The chelate was bound to a clay with its 3-fold symmetry axis at an angle of 60-65° with respect to the surface. No difference was observed for the orientations of the bound species between the racemic mixture and the pure enantiomer of the complex.

Introduction

We have been studying the adsorption of a metal complex by a clay, focusing our attention on the stereochemical effects on its bound states.[1,2] Metal complexes studied so far possess bulky planar ligands such as $[M(phen)_3]^{2+}$ and $[M(PAN)_3]^+$ (phen = 1,10-phenanthroline, and PAN = (1-pyridine-2-azo)-2-naphthol). It is found that the maximum adsorption amount is different when a metal complex is added as either a racemic mixture or a pure

* To whom correspondence should be addressed.

(1) Yamagishi, A.; Soma, M. *J. Am. Chem. Soc.* **1981**, *103*, 4640.
(2) Yamagishi, A. *J. Coord. Chem.* **1987**, *16*, 131.

0020-1669/91/1330-2462$02.50/0

enantiomer. The facts suggest that these complexes interact with their neighbors stereoselectively in the interlayer space.

The present paper reports the studies of the binding states of enantiomeric and racemic $[M(phen)_3]^{2+}$ with the methods of X-ray diffraction and electric dichroism measurements. The (00*l*) X-ray diffraction patterns for the powder samples of clay–chelate adducts give the electron density of a bound chelate along the *c* axis of a layer.

The electric dichroism measures the anisotropy in the electronic absorption of a chromophore in a solution by applying a high electric field pulse.[3] In the present case, a clay particle aligns with its bidimensional surface parallel with the electric field. When a light-absorbing molecule is bound to a clay particle, the anisotropy is induced in the wavelength region of the electronic absorption spectrum. From the magnitude of the induced dichroism at the complete orientation, the orientation of the transition moment due to a bound chromophore is determined with respect to the surface of a clay. It was intended to detect any difference in the orientation of the chelate when it was adsorbed as an enantiomer or a racemic mixture.

Experimental Section

Racemic and optically active $[M(phen)_3]Cl_2$ complexes (M = Fe(II) or Ru(II)) were prepared as described elsewhere.[4] The concentrations and optical purities of $[Ru(phen)_3]^{2+}$ were calculated from the electronic absorption spectra and circular dichroism spectra, using the following spectroscopic values: ϵ at 450 nm = 19 000 M^{-1} cm^{-1} and $\Delta\epsilon$ at 400 nm = −12 M^{-1} cm^{-1} for Λ-$[Ru(phen)_3]^{2+}$. The clay used was sodium montmorillonite purchased from Kunimine Industry Co. (Kunipia G). The elemental compositions were expressed as $[(Si_{7.20}Al_{0.80})(Mg_{5.97}Al_{0.03})O_{20}(OH)_4(Na_{0.76}K_{0.02}Ca_{0.07})]$. Its cation-exchange capacity (CEC) was 114 mequiv/g. A stock suspension of the clay was prepared by dispersing 0.114 g of the clay into 100 mL of water.

Electronic spectra were recorded on a spectrometer, UVIDEC 430 A (JASCO). The X-ray diffraction patterns and the intensities of the (00*l*) diffractions of powder samples were measured on the two-axis diffractometer (Rigaku). All of the X-ray diffraction data were processed and analyzed by the original programs on a micro-computer. The intensities from (001) to (008) diffractions were measured and reduced to the relative structure factors by the correction of the Lorentz–polarization factors.[8] Correction for the absorption was not carried out because the content of the heavy atom was not very large. The phases of the observed structural factors were determined from the calculations on the model structures. The structures of the clay–chelate adducts were assumed to be centrosymmetric. The atomic positions or the configuration of the chelate and the montmorillonite were taken from the reported structures of each compound.[13,14]

The electric dichroism was measured by applying an electric field pulse of 1 ms × 2 kV. The cell had an optical path length of 10 mm with an electrode separation of 6.0 mm. The electric field strength was changed by varying the electrode separation from 2.0 to 10.0 mm. The transmittance change was recorded in a transient memory, Wave Memory Model E-5001 (NF Circuit Design Block Co., Ltd.). The signal was read out on a recorder.

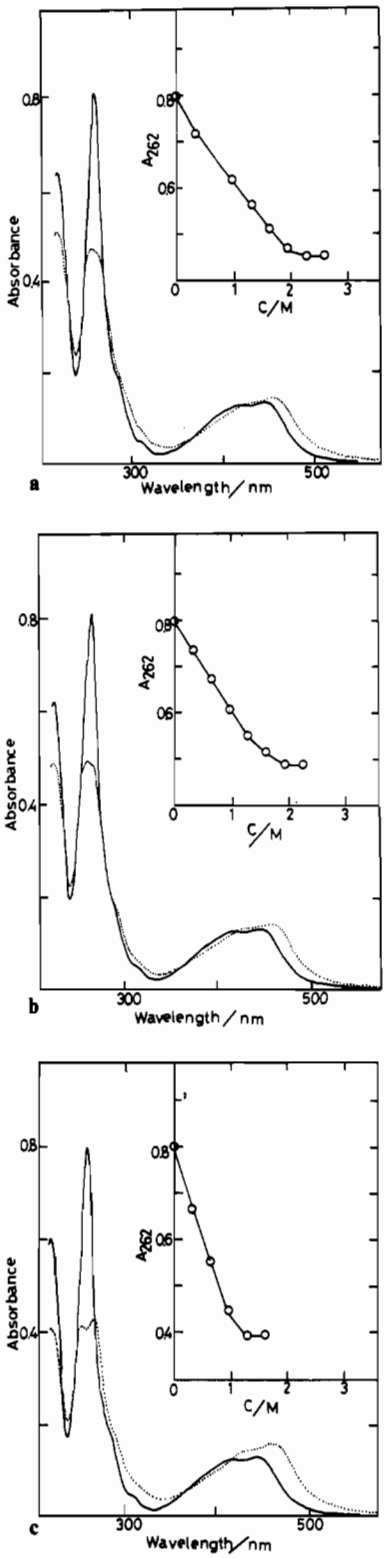

Figure 1. Electronic spectra of $[Ru(phen)_3]^{2+}$ in the absence of and in the presence of a colloidal clay: (a) Λ-$[Ru(phen)_3]^{2+}$ (7×10^{-6} M) and sodium montmorillonite (0 M for a solid line and 1.5×10^{-5} M for a dotted line); (b) *rac*-$[Ru(phen)_3]^{2+}$ (7×10^{-6} M) and sodium montmorillonite (0 M for a solid line and 1.5×10^{-5} for a dotted line); (c) *rac*-$[Ru(phen)_3]^{2+}$ (7×10^{-6} M), Na_2SO_4 (2.5×10^{-3} M), and sodium montmorillonite (0 M for a solid line and 8×10^{-6} M for a dotted line). The reference cell contained the same amount of a clay as the sample cell to cancel the effect of scattering of the light.

(3) Tricot, M.; Houssier, C. *Polyelectrolyte* Technomic Publishing Co. Inc.: Lancaster, PA, 1976; p 43.
(4) Dwyer, F. P. *Proc. R. Soc. N.S.W.* **1949**, *83*, 174.
(5) Loeppert, R. H.; Mortland, M. M.; Pinnavaia, T.J. *Clays Clay Miner.* **1979**, *27*, 201.
(6) McCaffery, A. J.; Mason, S. F.; Norman, B. J. *J. Chem. Soc. A* **1969**, 1428.
(7) (a) DellaGuardia, R. A.; Thomas, J. K. *J. Phys. Chem.* **1983**, *87*, 990. (b) Thomas, J. K. *Acc. Chem. Res.* **1988**, *21*, 275.
(8) The *Lp* factor: $F(000) = (\text{const})(I(\sin^2 s\theta)/(1 + \cos^2 2\theta))^{1/2}$, I = observed intensity, and const = constant. Cited from: *International Tables for X-ray Crystallography*; Kynoch Press: Birmingham, U.K., 1974; Vol. II, p 266.
(9) Dourlent, M.; Hogrel, J. F.; Helene, C. *J. Am. Chem. Soc.* **1974**, *96*, 3398.
(10) Yamagishi, A. *J. Phys. Chem.* **1984**, *88*, 5709.
(11) O'Konski, C. T.; Yoshioka, K.; Orttung, W. H. *J. Phys. Chem.* **1959**, *63*, 1558.
(12) Felix, F.; Ferguson, J.; Gudel, H. U.; Ludi, A. *Chem. Phys. Lett.* **1979**, *62*, 153.
(13) Recently it has been suggested that the excitation energy is localized on one of the ligands for $[Ru(bpy)_3]^{2+}$; e.g.: Myrick, M. L.; Blakley, R. L.; DeArmond, M. K.; Arthur, M. L. *J. Am. Chem. Soc.* **1988**, *110*, 1325.
(14) *Crystal Structures of Clay Minerals and their X-ray Identification*; Brindley, G. W., Brown, G., Eds.; Mineralogical Society: London, U.K., 1980.
(15) Zalkin, A.; Templeton, D. H.; Ueki, T. *Inorg. Chem.* **1973**, *12*, 1641.

For the adsorption measurements, a suspension of the clay and a metal complex was centrifuged at room temperature with a high-speed microrefrigerated centrifuge, Model MR-150 (TOMY). The amount of the adsorbed species was calculated from the decrease of the concentration in a supernatant solution after a suspension of the clay and a chelate was centrifuged at 15000 rpm for 1 h.

Results

(1) Study on the Adsorption of Enantiomeric and Racemic $[Ru(phen)_3]^{2+}$ by a Colloidal Clay. The adsorption of $[Ru(phen)_3]^{2+}$ by a colloidally dispersed clay was studied by measurement of electronic absorption spectra. The electronic spectra were measured for the following three samples: (i) the clay was added to a solution of enantiomeric $[Ru(phen)_3]^{2+}$, (ii) the clay was added to a solution of racemic $[Ru(phen)_3]^{2+}$, and (iii) the clay was added to a solution of racemic $[Ru(phen)_3]^{2+}$ in the presence of 2.5 mM of Na_2SO_4. In the first two cases, no electrolyte was added to a solution. For case iii, Na_2SO_4 was added as an electrolyte since it was previously reported that doubly charged negative anions were effective to achieve the adsorption of racemic $[Fe(phen)_3]^{2+}$ in excess over the cation-exchange capacity (CEC) of a clay.[5]

The dotted curves in parts a–c of Figure 1 are the spectra for cases i–iii, respectively, where the clay had been added until the solutions showed no further change in the electronic spectra. The absorption in the wavelength region 240–280 nm was due to local excitations of the phenanthroline ligands.[6] For all three cases, that absorption band decreased on adding a clay. A similar change was reported for the adsorption of $[Ru(bpy)_3]^{2+}$ (bpy = 2,2′-bipyridine).[7]

The absorbance at 262 nm, A_{262}, was plotted against the ratio of [clay] to [chelate], in which the concentration of a clay was measured in terms of the CEC. The results are shown in the inserted graphs in Figure 1a–c. A_{262} decreased almost linearly until it leveled off at the approximate values of [clay]/[chelate] = 2, 2, and 1 for cases i–iii, respectively. The total absorbance change on adsorption was nearly the same for all three cases.

The absorption band in the wavelength range 350–500 nm was ascribed to the charge-transfer transition from the d electrons of Ru(II) to the π^* orbitals of the ligands.[6] This band displaced toward the longer wavelength on adsorption in the above three cases. The total absorbance change at 475 nm per molecule was the largest for case iii among the investigated three cases. Since the surface density of the adsorbed chelates was the largest for case iii, the high intermolecular interlaction for case iii was considered to cause the largest absorbance change at 475 nm.

The adsorption of the chelate was also studied by use of the change of the absorbance at 475 nm, A_{475}. A_{475} was plotted against the ratio of clay to chelate in a similar way. In these plots, A_{475} continued to increase until [clay]/[chelate] attained the values of 2, 2, and 1 for cases i–iii, respectively.

On the basis of the above results, it was derived that the chelate was adsorbed, occupying two cation-exchange sites per molecule for cases i and ii. Since the chelate carried two positive charges, it was adsorbed within the CEC of a clay

$$[Ru(phen)_3]^{2+} + 2M^- \rightarrow [Ru(phen)_3]^{2+}\cdot 2M^- \quad (1)$$

where M^- denotes the cation-exchange site of a clay.

On the contrary, in case iii, the chelate was adsorbed, occupying one cation-exchange site per molecule, or it was adsorbed by a 2-fold excess of CEC:

$$[Ru(phen)_3]^{2+} + M^- \rightarrow [Ru(phen)_3]^{2+}\cdot M^- \quad (2)$$

The difference between cases ii and iii lay in the fact that an electrolyte, Na_2SO_4, was present in the latter case. Previous experiments reporting the excess adsorption of *rac*-$[Fe(phen)_3]$ were performed in the concentration range of a chelate from 0.1 to 1 mM.[1] Under such conditions, the concentration of the counteranions in the added chelates was high enough to achieve the racemic adsorption without adding electrolytes.

Finally, the adsorption of enantiomeric $[Ru(phen)_3]^{2+}$ was studied in the presence of an electrolyte, 2.5 mM of Na_2SO_4. In this case, no excess adsorption over CEC was observed. Thus the enantiomeric chelate was adsorbed, occupying two cation exchange sites per molecule in the presence of an electrolyte.

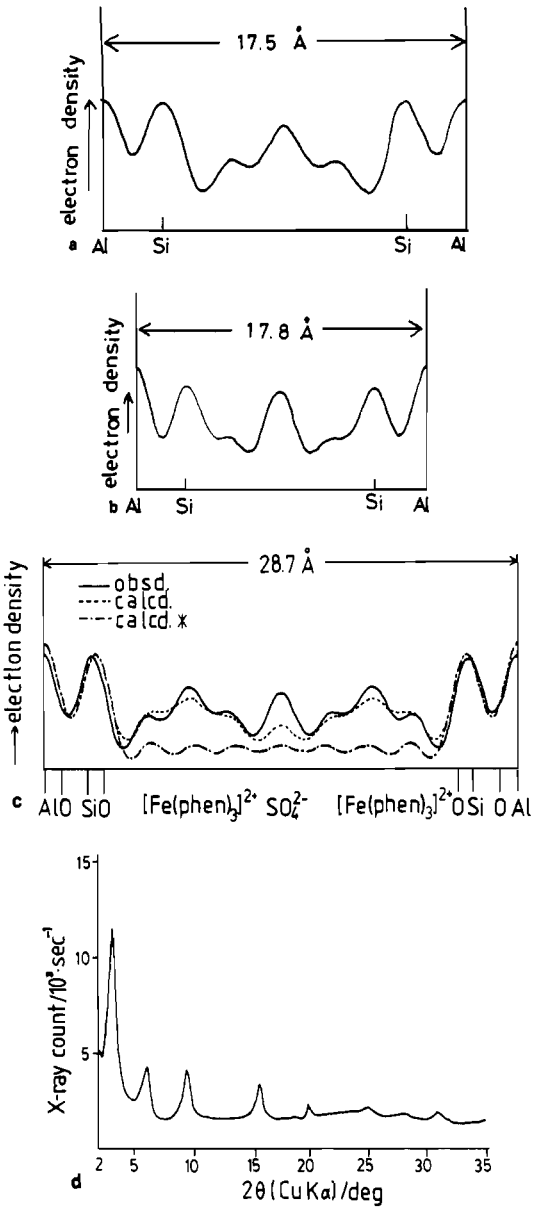

Figure 2. Electron density curves of clay–chelate adducts: (a) 2:1 clay–Λ-$[Ru(phen)_3]^{2+}$; (b) 2:1 clay–*rac*-$[Fe(phen)_3]^{2+}$; (c) 1:1 clay–*rac*-$[Fe(phen)_3]^{2+}$ (—, - - -) and a clay only (–·–). (d) Raw diffraction data for part c.

(2) X-ray Diffraction Studies of the Adduct of the Clay and a Chelate. The X-ray diffraction was measured for the powder samples of 2:1 and 1:1 clay–$[M(phen)_3]^{2+}$ for M = Ru and Fe. Here 2:1 and 1:1 denoted that the ratio of a clay in CEC to a chelate in moles was 2:1 and 1:1, respectively.

Table I gives the basal spacings of these samples that were obtained from the (001) values. Since the basal spacing of sodium montmorillonite (12.9 Å) was expanded by 5–16 Å for all the chelate–clay adducts, the chelates were confirmed to be intercalated between the clay layers.

The intensities from (001) to (008) diffractions were measured and reduced to the relative structure factors by the correction of the Lorentz–polarization factors.[8] Correction of the absorption was not carried out because the content of the heavy atom was not so large. By Fourier transformation, the electron distributions along the *c* axis were obtained for the cases of 2:1 clay –Λ-$[Ru(phen)_3]^{2+}$, 2:1 clay–*rac*-$[Fe(phen)_3]^{2+}$ and 1:1 clay–racemic $[Fe(phen)_3]^{2+}$. The results are displayed in Figure 2 a–c together with the raw powder diffraction data in Figure 2d. In Figure 2c,

Table I. Basal Spacings (001) of Clay–Chelate Adducts

cation	% cation exchange vs CEC	(001) spacing, Å
Na^+	100	12.9
Λ-$[Ru(phen)_3]^{2+}$	100	17.8
rac-$[Fe(phen)_3]^{2+}$	100	17.8
rac-$[Fe(phen)_3]^{2+}$	170	28.7
rac-$[Ru(phen)_3]^{2+}$	160	29.7

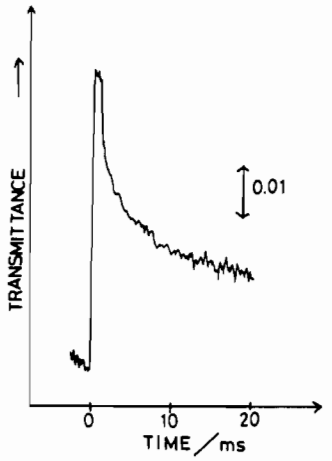

Figure 3. Electric dichroism signal for a suspension of Λ-$[Ru(phen)_3]^{2+}$ (7×10^{-6} M) and clay (3×10^{-5} M). Wavelength as 450 nm.

the electron distribution of a clay that does not contain the chelates is included.

For both 2:1 clay–Λ-$[Ru(phen)_3]^{2+}$ and 2:1 clay–*rac*-$[Fe(phen)_3]^{2+}$, one peak existed in the middle of the interlayer space. The peak is apparently ascribed to the intercalated metal chelate. For 1:1 clay–*rac*-$[Fe(phen)_3]^{2+}$, two large peaks existed in the interlayer region with one small peak between them. The large two peaks were ascribed to the Fe chelates, while one small peak in the middle was due to the anion, SO_4^{2-}. The anion was intercalated in order to compensate the excess positive charge caused by the adsorption of cations in excess over the CEC.

In the sample used to obtain Figure 2c, the chelates were presumed to be present in the form of a racemic compound. The steric interaction between the upper and lower adsorbate layers might be prohibited by the presence of the intervening anions. Accordingly the stereoselective interaction leading to the formation of the racemic compound was most probably operative within each of the adsorbate layers.

(3) Electric Dichroism Measurements of a Clay–Chelate Suspension. Electric dichroism was measured for a colloidal suspension of an adduct of a clay and a chelate. Measurements were performed for the following samples: (1) a suspension containing 3×10^{-5} M of a clay and 7×10^{-6} M of Λ-$[Ru(phen)_3]^{2+}$; (2) a suspension containing 1.5×10^{-5} M of a clay and 7×10^{-6} M of *rac*-$[Ru(phen)_3]^{2+}$ in the presence of a 1 mM of Na_2SO_4.

Figure 3 shows an example of the electric dichroism signal for sample 1. When an electric field of 3.3 kV/cm was applied for a duration of 1 ms, the transmittance at 450 nm increased to attain the sationary value within 0.1 ms. The signal decayed to the initial transmittance level about 500 ms after the applied field was turned off. The relative amplitude of the signal depended on the angle between the electric field and the polarization of the monitoring light, α

$$\Delta A/A = (\rho/6)\,(3\cos 2\alpha + 1) \qquad (3)$$

in which A is the absorbance in the absence of the electric field and ΔA is the amplitude of the signal, respectively. ρ is reduced linear dichroism defined as[9]

$$\rho = (\epsilon_\parallel - \epsilon_\perp)/\epsilon \qquad (4)$$

in which ϵ, $\epsilon_\parallel$, and $\epsilon_\perp$ are an isotropic extinction coefficient, an extinction coefficient for parallel polarized light and an extinction coefficient for perpendicularly polarized light, respectively.

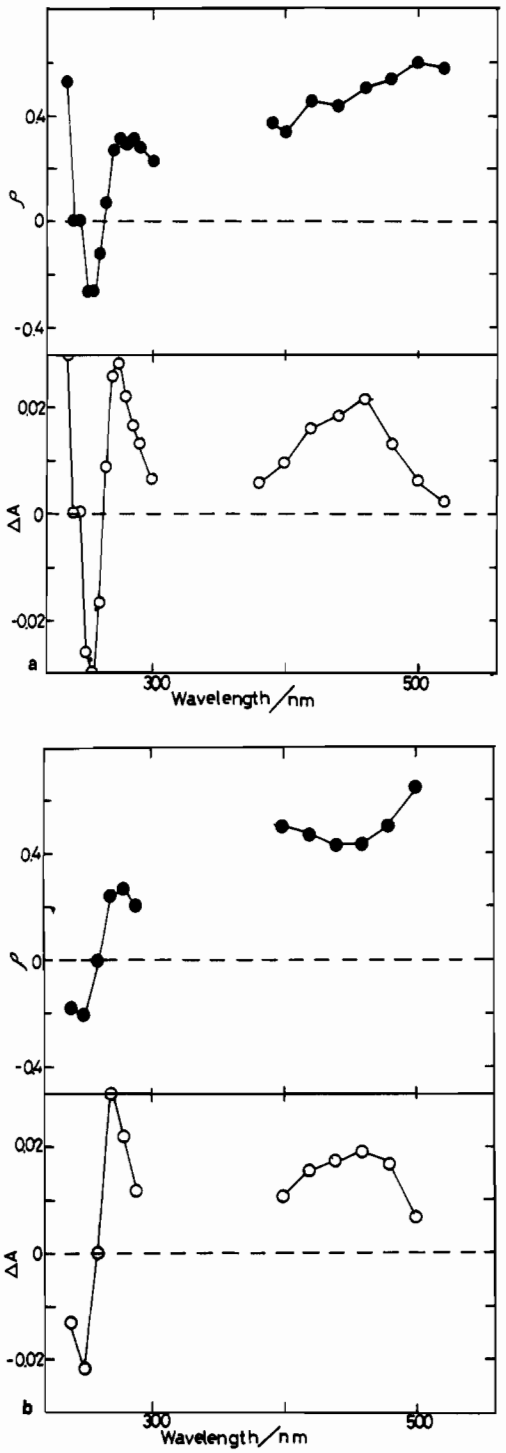

Figure 4. Dependences of the reduced linear dichroisms on the wavelength of monitoring light: (a) for a suspension of Λ-$[Ru(phen)_3]^{2+}$ and clay; and (b) for a suspension of *rac*-$[Ru(phen)_3]^{2+}$ and clay. The amplitude of the electric dichroism was measured for the light polarized in parallel with the electric field.

Parts a and b of Figure 4 show the dependences of the dichroism amplitudes and the reduced linear dichroisms on the wavelength of the monitoring light for samples 1 and 2, respectively.

In the present systems, a chromophore was located on a bidimensional surface of a clay. If the bound molecule orientated its transition moment at an angle, ψ, with respect to the surface, the reduced linear dichroism is related to the angle, ψ[10]

$$\rho = (-3/8)(1 + 3\cos 2\psi)\cdot\Phi(E) \qquad (5)$$

in which $\Phi(E)$ is an orientation function representing the degree of the orientation of a macromolecule under the electric field.[11] The above equation was derived by averaging out the orientation

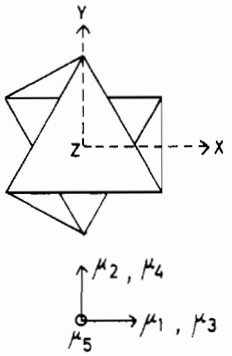

Figure 5. Orientation of the transition moments for the charge-transfer absorption band (μ_1, μ_2) and for the local excitation band (μ_3, μ_4, μ_5) in a $[Ru(phen)_3]^{2+}$ molecule. μ_1 and μ_3 lie along the x axis, μ_2 and μ_4 lie along the y axis, and μ_5 lies along the z axis, respectively.

Table II. Reduced Linear Dichroisms of Bound $[Ru(phen)_3]^{2+}$ Chelate

	reduced linear dichroism				
	MLCT band		local excitation		
complex	μ_1	μ_2	μ_3	μ_4	μ_5
rac-$[Ru(phen)_3]^{2+}$	0.50	0.42	0.25		−0.20
Λ-$[Ru(phen)_3]^{2+}$	0.60	0.45	0.35		−0.28
calcd (θ = 25°; ϕ = 0°)	0.47	0.47	0.47	0.47	−0.94
(θ = 30°; ϕ = 0°)	0.55	0.55	0.55	0.55	−1.01

of the transition moment over 360° on the surface, keeping the angle with respect to the surface at ψ. In the present experiments, the orientation function was regarded as 1, because the amplitude of the induced dichroism was constant with an increase of the electric field strength from 1 to 10 kV/cm.

The absorption band in the visible region of $[Ru(phen)_3]^{2+}$ was assigned to the metal-to-ligand charge-transfer transition from the d electrons of Ru(II) to the π^* orbitals of the ligands (MLCT).[6] Due to the 3-fold symmetry of the present chelate, the band mainly contained two different kinds of transitions: one involved the excitation to the π^* orbital that is symmetric with respect to the 2-fold symmetric axis of a ligand (μ_1) and the other involved the excitation to the π^* orbital antisymmetric with respect to that axis (μ_2).[12] Here it was assumed that the same arguments were applied to the nature of the electronic transition for both $[Ru(bpy)_3]^{2+}$ and $[Ru(phen)_3]^{2+}$. Accordingly the peaks at 400 and 450 nm in the electronic spectrum were assigned to the transitions from the d orbital of Ru(II) to the antisymmetric and symmetric excited states of the ligand, respectively.[12] These assignments are based on the model where the excitation energy is completely delocalized among the three ligands.[13] The transition moments for these peaks lie on the plane perpendicular to the 3-fold symmetry axis and are orientated in the molecule as shown in Figure 5. If the chelate still maintained the 3-fold symmetry in the bound state, there are two other equivalent orientations for these transition moments due to that symmetry.

The absorption bands at 230–280 nm arose from the local excitation in the ligands.[6] There are three independent transition moments in these bands. Two of them are on the plane perpendicular to the 3-fold symmetry axis, one (μ_3) symmetric and the other (μ_4) antisymmetric with respect to the 2-fold symmetry axis. The third (μ_5) is parallel with the 3-fold symmetry axis. The orientations of them are shown also in Figure 5. There also exist two more equivalent orientations for these transitions due to the 3-fold symmetry of the complex.

From the results in Figure 4a,b, the observed values of the reduced linear dichroisms were obtained for the bound enantiomeric and racemic $[Ru(phen)_3]^{2+}$ as tabulated in Table II. In order to determine the possible orientations of the bound chelates, these observed values were compared with the calculated ones for a chelate in various orientations.

Parts a and b of Figure 6 show the calculated results for the reduced linear dichroisms due to the symmetric (μ_1 and μ_3) and

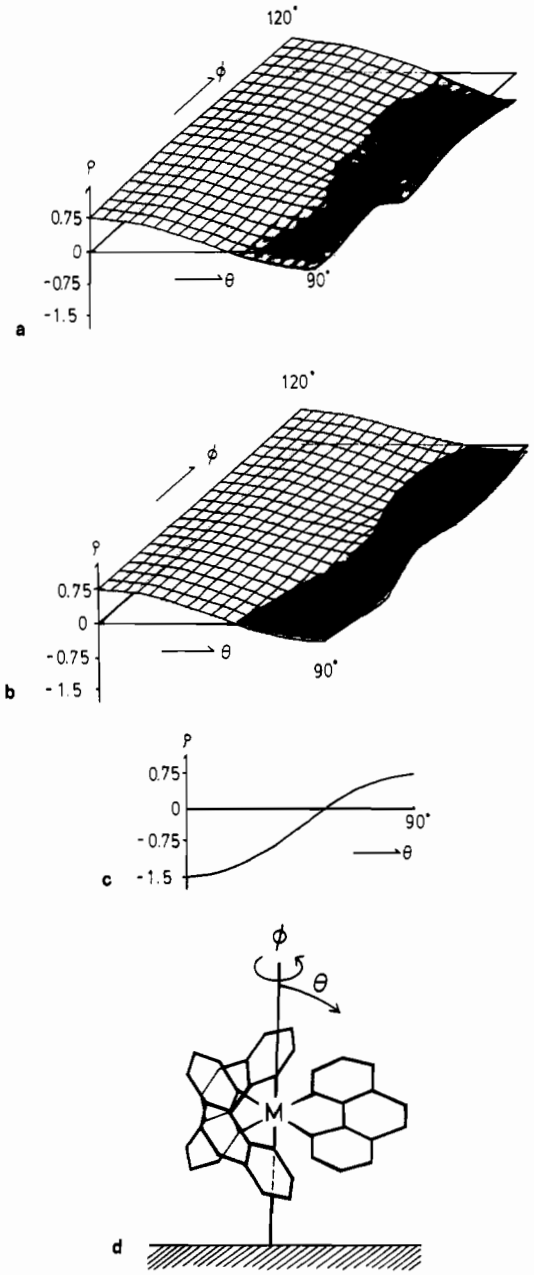

Figure 6. Dependences of the reduced linear dichroisms on the molecular orientation of $[Ru(phen)_3]^{2+}$. (a) Mean value of the reduced linear dichroisms of three equivalent symmetric transition moments (μ_1 and μ_3). (b) Mean value of the reduced linear dichroisms of three equivalent antisymmetric transition moments (μ_2 and μ_4). (c) Dependence of the reduced linear dichroism of transition moment μ_5 on the θ angle. (d) Parameters describing the orientation of the chelate.

antisymmetric transitions (μ_2 and μ_4) that are perpendicular to the 3-fold symmetry axis in both the charge-transfer and local excitation bands, respectively. Figure 6c shows the dependence of the reduced linear dichroism of the transition moment (μ_5), which is parallel with the 3-fold symmetry axis in the local excitation band, on the angle, θ, between the 3-fold symmetry axis and the vertical direction with respect to the clay surface. Here the orientation parameters were chosen as shown in Figure 6d.

We sought the orientation of a bound chelate that reproduced the observed reduced linear dichroisms as well as possible. As for the charge-transfer region, the reduced dichroism was positive, showing little dependence on the wavelength. This implies that the two transition moments, μ_1 and μ_2, that were vertical to each other were orientated in almost the same angle with respect to the clay surface.

On the other hand, the reduced linear dichroism in the local excitation region had clearly two peaks with opposite signs. The

negative peak of linear dichroism at 250 nm was assigned to the transition moment, μ_5, that was parallel with the 3-fold symmetry axis and the positive peak at 270 nm to the two transition moments, μ_3 and μ_4, that were perpendicular to the 3-fold symmetry axis.

Table II includes the orientation that leads to the best coincidence between the observed and calculated magnitudes of the reduced linear dichroisms. The agreement between the observed and calculated values are not very good, especially for the local excitation bands. One of the reasons for such a discrepancy might lie in the facts that the chelates did not have the definite value of the angle, θ, but they orientated their transition moments in some range of the angle. It is, however, not possible to estimate the distribution function of the angle, θ, by the present methods. The large discrepancy in the local excitation bands might also be caused by the low resolution of wavelength (ca. 5 nm) so that the two oppositely signed peaks overlapped to cancel out each other. This effect resulted in the significant decrease of the absolute magnitudes of the reduced linear dichroisms. At present, we were forced to be satisfied with the approximate conclusion that the chelate was bound to a clay with its 3-fold symmetry axis at an angle of 65–60° with respect to the clay surface. There was no observable difference between the bound states of the enantiomers and racemic chelates.

Discussion

The maximum amount of adsorption of $[Ru(phen)_3]^{2+}$ was compared for the enantiomer and the racemic mixture in the presence of Na_2SO_4 (2.5 mM). It was confirmed that the racemic mixtures were adsorbed to almost a 2 times excess of the CEC of a clay, while the enantiomers were adsorbed within the CEC.

From the X-ray diffraction analyses, it was observed that the racemic mixtures formed a double-molecular layer with intervening SO_4^{2-} ions in the interlayer spaces. In contrast, the enantiomers formed a single molecular layer with no SO_4^{2-} included in the adduct.

The present $[M(phen)_3]^{2+}$ molecule is regarded as a sphere with a radius of about 4 Å. When it is adsorbed on a silicate sheet, it roughly occupies three hexagonal holes surrounded by six $[SiO_4]^{2-}$ tetrahedrons. In this sense, the area covered by the neighboring three hexagonal holes is denoted as a "site". From the elemental compositions of the present clay sample (see Experimental Section), every site possesses the negative charge of −1.3. Thus one site accepts 1.3 molecules at the adsorption of a 2 times excess of CEC. Since at most a single molecule is accommodated within the site, the rest of the molecule or 0.3 part out of 1.3 (23% of the whole chelate) should form another adsorbate layer. This is the reason that the racemic mixture forms a double layer in the interlayer space.

The fact that the excess adsorption was observed exclusively for the racemic mixture but not for the pure enantiomer suggested that they formed the racemic compound in the bound state. In other words, an enantiomer and its antipode interacted stereoselectively to form a stereoregular adsorbate layer.

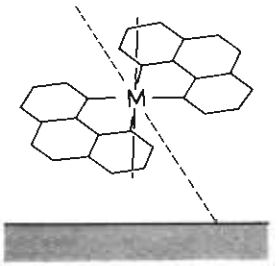

Figure 7. Possible binding structure of $[Ru(phen)_3]^{2+}$ intercalated in the clay layers.

In the double layer of adsorbed racemic chelates, the molecules in the upper and lower layers interacted sterically to a negligible extent. This is expected because an anion is located between these two layers. Accordingly, the stereoselective interaction to realize the racemic adsorption might be operative within each of the upper and lower layers. No structural conclusion as to the intermolecular interaction was, however, derived from the present X-ray diffraction measurements.

From the electric dichroism measurements, the orientation of bound $[Ru(phen)_3]^{2+}$ was determined. As a result, the 3-fold symmetry axis was found to decline by about 25–30° from the vertical direction on a clay surface. No distinct difference was observed as to the orientations between the racemic mixture and the pure enantiomer. The difference in the maximum adsorption amounts between these two was therefore ascribed to the intermolecular interaction among the bound chelates but not to the interaction of the individual molecules with a clay surface.

The dichroism results as to the local excitation bands of the coordinated ligands confirmed that the two split peaks in this region were due to the different transition moments, one (at the shorter wavelength) orienting in the direction parallel with the 3-fold symmetry axis and the other in the direction perpendicular to the axis. These transitions were optically active and gave rise to two peaks with opposite signs.[6] The magnitude of the splitting between the two peaks is determined by the electronic interaction between the ligands.[6] Accordingly, the larger splitting observed in the racemic adsorption indicated that the chelate was deformed so as to increase the interligand interaction.

The structure of the bound $[Ru(phen)_3]^{2+}$ deduced from the dichroism measurements is drawn in Figure 7. In this orientation, one of the ligands makes almost a vertical angle with respect to the clay surface. When the molecule is adsorbed on a single clay layer, it is expected to be adsorbed with its 3-fold symmetry axis perpendicular to the surface. This configuration is considered to be most stable since the positive metal center is closest to the surface. Therefore, it is suspected that the decline of the symmetry axis by an angle of 25–30 ° is caused by the simultaneous interaction of the chelate with the upper and lower surfaces. No detailed mechanism for the inclination of the axis is clear at the present stage.